Cell Reports

Adaptive Evolution of MERS-CoV to Species Variation in DPP4

Graphical Abstract

Highlights

- MERS-CoV infected cells expressing DPP4 from 16 bat species

- MERS-CoV spike rapidly adapted to species variation in DPP4

- Viral adaptations modified the surface charge of viral spike

- Different routes of spike adaptation enhanced entry with the same DPP4 variant
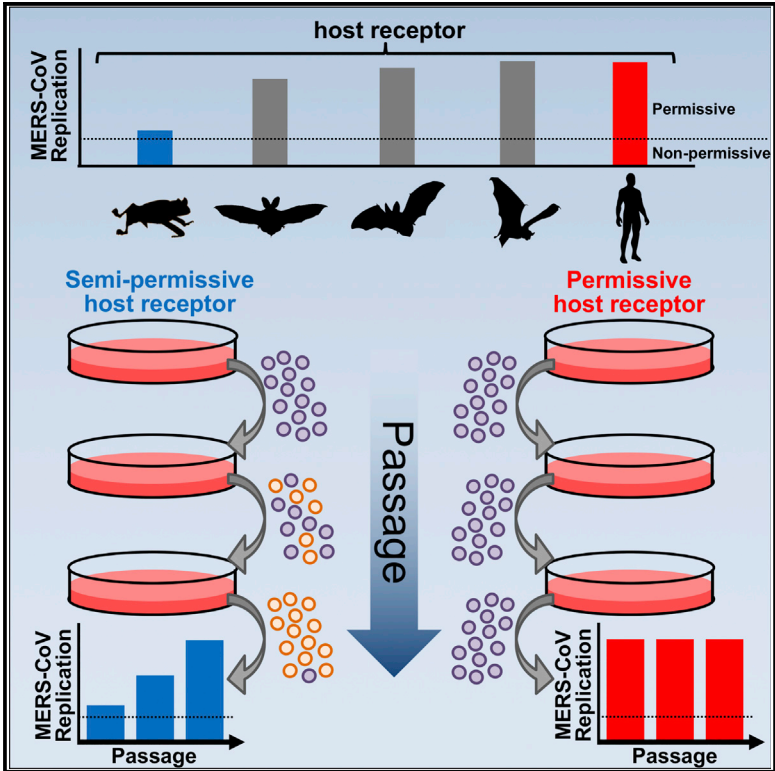
Authors

Michael Letko, Kerri Miazgowicz, Rebekah McMinn, ..., Aaron Carmody, Neeltje van Doremalen, Vincent Munster

Correspondence

michael.letko@nih.gov (M.L.), vincent.munster@nih.gov (V.M.)

In Brief

MERS-CoV is a zoonotic pathogen capable of infecting numerous species. However, our understanding of how this virus adapts to new species remains unclear. Letko et al. experimentally observe several different routes in the stepwise, adaptive evolution of MERS-CoV to a unique host-species variant of the viral receptor.

CellPress

Adaptive Evolution of MERS-CoV to Species Variation in DPP4

Michael Letko,[1,6,*] Kerri Miazgowicz,[1,3,6] Rebekah McMinn,[1,4] Stephanie N. Seifert,[1] Isabel Sola,[5] Luis Enjuanes,[5] Aaron Carmody,[2] Neeltje van Doremalen,[1] and Vincent Munster[1,7,*]

[1]Laboratory of Virology, Division of Intramural Research, National Institute of Allergy and Infectious Diseases, National Institutes of Health, Hamilton, MT 59840, USA
[2]Research Technologies Branch, Rocky Mountain Laboratories, National Institute of Allergy and Infectious Diseases, National Institutes of Health, Hamilton, MT 59840, USA
[3]Department of Infectious Diseases, College of Veterinary Medicine, The University of Georgia, Athens, GA 30602, USA
[4]Department of Microbiology, Immunology, & Pathology, Colorado State University, Fort Collins, CO 80523, USA
[5]Department of Molecular and Cell Biology, Centro Nacional de Biotecnología (CNB-CSIC), Campus Universidad Autónoma de Madrid, Cantoblanco, Madrid, Spain
[6]These authors contributed equally
[7]Lead Contact
*Correspondence: michael.letko@nih.gov (M.L.), vincent.munster@nih.gov (V.M.)
https://doi.org/10.1016/j.celrep.2018.07.045

SUMMARY

Middle East Respiratory Syndrome Coronavirus (MERS-CoV) likely originated in bats and passed to humans through dromedary camels; however, the genetic mechanisms underlying cross-species adaptation remain poorly understood. Variation in the host receptor, dipeptidyl peptidase 4 (DPP4), can block the interaction with the MERS-CoV spike protein and form a species barrier to infection. To better understand the species adaptability of MERS-CoV, we identified a suboptimal species-derived variant of DPP4 to study viral adaption. Passaging virus on cells expressing this DPP4 variant led to accumulation of mutations in the viral spike which increased replication. Parallel passages revealed distinct paths of viral adaptation to the same DPP4 variant. Structural analysis and functional assays showed that these mutations enhanced viral entry with suboptimal DPP4 by altering the surface charge of spike. These findings demonstrate that MERS-CoV spike can utilize multiple paths to rapidly adapt to novel species variation in DPP4.

INTRODUCTION

Since its discovery in 2012, Middle East Respiratory Syndrome Coronavirus (MERS-CoV) has infected over 2,000 people and has a mortality rate of approximately 35% (World Health Organization, 2018WHO; Zaki et al., 2012). The ancestral host species of MERS-CoV remains elusive; however, mounting evidence suggests that the virus most likely originated in bats and passed to humans through multiple zoonotic spill-over events from dromedary camels (Azhar et al., 2014; Haagmans et al., 2014; Ithete et al., 2013; Woo et al., 2012). While species capable of supporting MERS-CoV infection have been studied, the genetic

mechanisms underlying cross-species adaptation remain poorly understood.

A primary determinant of viral species-tropism is at the level of host cell entry, which is mediated by MERS-CoV spike protein binding host dipeptidyl peptidase 4 (DPP4) (Ohnuma et al., 2013; Raj et al., 2013). Structural studies have shown that this interaction relies on multiple contact points (Lu et al., 2013; Song et al., 2014; Wang et al., 2013). Our group has previously demonstrated that hamster DPP4 contains variation in these contact points, which prevents MERS-CoV replication (van Doremalen et al., 2014; van Doremalen et al., 2016). Other genetic variation responsible for the glycosylation of DPP4 in mice, hamsters, ferrets, and guinea pigs forms an additional block to the interaction with MERS-CoV spike (Cockrell et al., 2014; Peck et al., 2017). In contrast to small rodents and ferrets, MERS-CoV is capable of utilizing DPP4 from different bat species, and *Artibeus jamaicensis* bats have been shown to support experimental infection (Caì et al., 2014; Munster et al., 2016).

Here, we investigated the host breadth and adaptability of MERS-CoV. We demonstrate that MERS-CoV can use DPP4 from a diverse range of bat species and can rapidly adapt to variation in DPP4.

RESULTS

Identification of a Semi-Permissive DPP4 Variant

We selected 16 bat species representing a broad taxonomic and geographic distribution to screen for MERS-CoV entry (Figures 1A, S1, and S2). Plasmids encoding the bat DPP4s were transfected into Baby Hamster Kidney fibroblasts (BHK) cells, which are non-permissive to MERS-CoV infection (van Doremalen et al., 2014). All DPP4s supported viral replication to varying degrees; however, *Desmodus rotundus* DPP4 (*dr*DPP4) was the least permissive to viral replication (Figure 1B). Flow cytometry showed that DPP4 surface expression varied between species but did not correlate with infectivity (Figure S3A). While this may result from variation in antibody recognition, to date, no
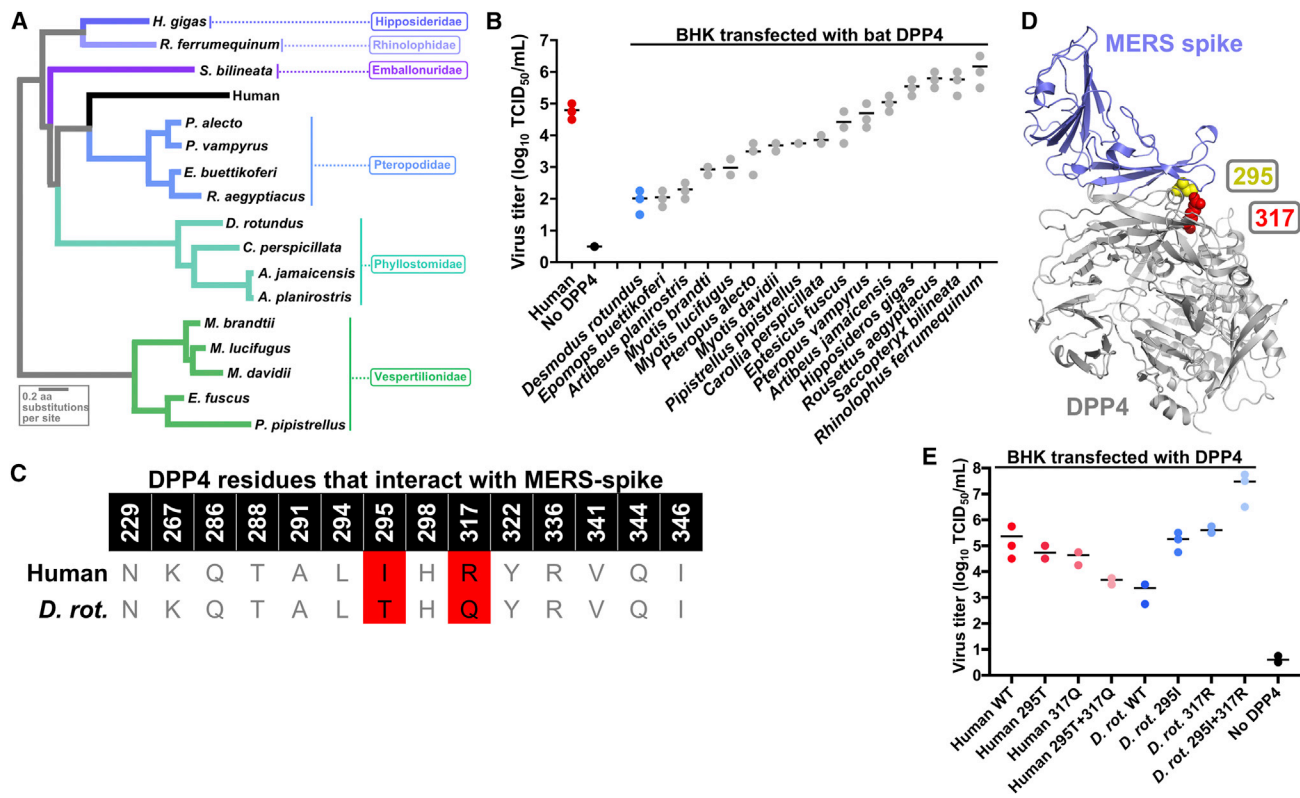
Figure 1. *Desmodus Rotundus* DPP4 Is Semi-Permissive for MERS-CoV Replication

(A) Phylogenetic tree of the DPP4 amino acid sequences used in this study. See also Figures S1 and S2.

(B) BHK cells were transfected with equivalent amounts of bat-DPP4 expression plasmids. Cells were infected 24 hr later with MERS-CoV at MOI = 1. Viral titer of 48-hr supernatants was determined by titration on Vero cells. Each dot on the graph represents one replicate and horizontal black lines represent the mean of three replicates. See also Figure S3A.

(C) Comparison of MERS-spike binding residues between human and *Desmodus rotundus* DPP4. See also Figure S3B.

(D) Structure of MERS-CoV spike protein bound to human DPP4 (PDB: 4L72) with DPP4 residues 295 and 317 indicated in yellow and red, respectively.

(E) Human and *dr*DPP4-295 and 317 mutants were transfected in BHK cells. Cells were infected 24 hr later with MERS-CoV at MOI = 1. Viral titer of 48-hr supernatants was determined by titration on Vero cells. Each dot on the graph represents one replicate, and horizontal black lines represent the mean of three replicates.

commercially available DPP4 antibody recognizes an epitope that is conserved across all species.

Relative to human DPP4, the bat DPP4s contained variation throughout the whole spike-binding region (Figure S3B). However, within the residues, which specifically bind MERS-CoV spike, *dr*DPP4 only differed from human DPP4 in two amino acids at positions 295 and 317 (Figures 1C, 1D, and S3B) (Wang et al., 2013). As *dr*DPP4 was also unique at position 317 (R317Q), we chose to focus on *dr*DPP4. Introducing *dr*DPP4 mutations into human DPP4 reduced viral replication, while mutating *dr*DPP4 to match the amino acids in human DPP4 increased its ability to support MERS-CoV replication (Figure 1E). These data show that residues 295 and 317 largely determine resistance of *dr*DPP4 to MERS-CoV replication.

Viral Adaptation of MERS-CoV to *Desmodus Rotundus* DPP4

As only two *dr*DPP4 residues influenced MERS-CoV replication, we hypothesized that viral spike may be able to adapt to this vari-

ation. To test this, we generated BHK cell lines that stably expressed human DPP4, *dr*DPP4, or blue fluorescent protein (BFP; a negative control) from a lentiviral expression cassette that also included a fluorescent reporter, mCherry, as well as a puromycin selection gene (Figure 2A). These genes were separated by 2A sequences, which allowed for all three to express under the human Ef1α promoter (Letko et al., 2015). Flow cytometry for mCherry and DPP4 confirmed similar transduction efficiency and transgene expression levels, respectively, between human and *dr*DPP4 cell lines (Figure 2B). Cells expressing *dr*DPP4 were less susceptible than human DPP4 to MERS-CoV infection, similar to our transfection experiments (Figure 2C).

Wild-type (WT) MERS-CoV was serially passaged, in triplicate, on these DPP4 and control cell lines. While human DPP4 cells showed cytopathic effects (CPE) from the first passage, *dr*DPP4 cells only showed CPE after eight passages, indicative of viral adaptation (Figure 2D). Sanger sequencing of the MERS-CoV spike receptor binding domain (RBD) revealed the emergence of several mutations with the *dr*DPP4 cell cultures (Figure 2E).
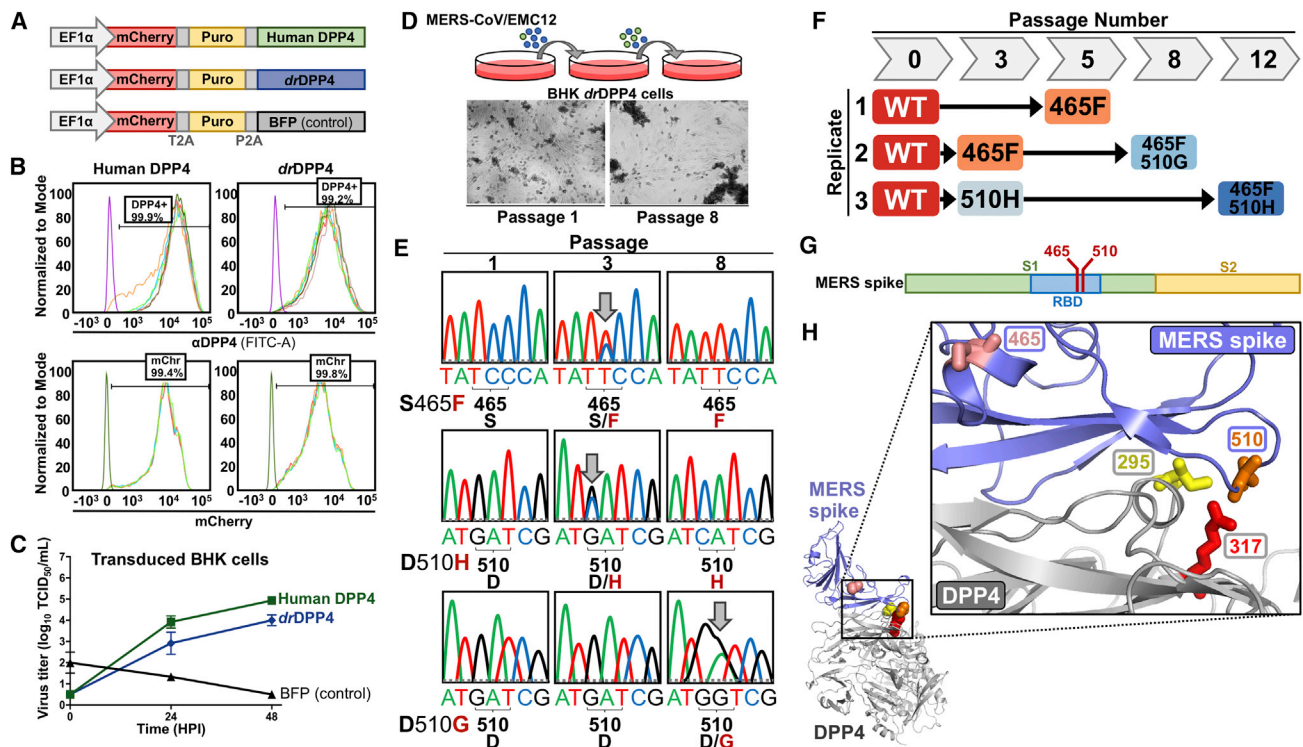
Figure 2. Forced Adaptation of MERS-CoV on DPP4 Stable Cell Lines

(A) An overview of the lentiviral expression cassette.

(B) Flow cytometry of transduced cells.

(C) Transduced cells were infected with MERS-CoV at MOI = 0.001. Viral titer was determined by titration on Vero cells. Error bars represent the SDs of three replicates.

(D) MERS-CoV was passaged on DPP4-tansduced cells. Cytopathic effects were observed by passage 8.

(E) Sequencing chromatograms of MERS-CoV spike from different passages on the *dr*DPP4 cells. Arrows indicate emerging mutations (overlapping peaks).

(F) Schematic of single and double mutation emergence in MERS-CoV spike over different passages. See also Figure S4A.

(G) Location of mutations within MERS-CoV spike.

(H) Location of mutations in the MERS-CoV spike co-structure with human DPP4 (PDB: 4L72). MERS-CoV spike is colored blue and residues 465 and 510 are shown in pink and orange, respectively. DPP4 is colored gray and residues 295 and 317 are shown in yellow and red, respectively.

By the fifth passage, spike S465F emerged in two replicates, and spike D510H emerged in one replicate (Figure 2F). By passage 8, one S465F mutant acquired a secondary D510G mutation, and on passage 12, the D510H mutant acquired a secondary S465F mutation (Figure 2F). We sequenced the spike RBD from 14 passages, as well as full-length spike from passages 3, 6, and 9, but did not observe additional mutations. No spike mutations were observed with the human DPP4 or control cell lines, indicating that these mutations were specific for *dr*DPP4 and not the BHK cells themselves. Spike residues 465 and 510 are located within the RBD and interface with DPP4 (Figures 2G and 2H). Notably, spike residue 510 clusters with DPP4 residues 295 and 317 and directly interacts with DPP4 residue 317 (Figure 2H) (Wang et al., 2013). MERS spike 465S and 510D are found in the majority of published spike sequences (Figure S4A).

Characterization of MERS-CoV Spike Mutations

Human and *dr*DPP4 are 83.8% similar at the amino acid level and both function as the receptor for MERS-CoV, suggesting the two proteins share a common structure. Therefore, we used struc-

tural data for human DPP4 to predict the structure of *dr*DPP4. Electrostatic potential analysis showed a positive surface charge of human DPP4 at residues 295 and 317 and a negative charge at these positions in *dr*DPP4 (Figure 3A). Complementary to human DPP4, the WT MERS-CoV spike RBD is negatively charged (Figure 3B). This analysis revealed that the spike adaptations altered the surface charge of spike from negative to positive, complementing the negative charge of *dr*DPP4 (Figure 3C).

Because we only sequenced MERS-CoV spike, it remained possible that other mutations arose in the viral genome that increased viral replication in the *dr*DPP4 cells. Therefore, we generated spike point mutant viruses, which failed to grow on control transduced cells but grew to similar levels as WT virus and induced CPE in the human DPP4 cells (Figures 3D and S4B). In contrast, WT virus replicated to lower titers than the spike mutants and failed to induce CPE in *dr*DPP4 cells (Figures 3D and S4B). Next, we performed an entry assay with spike-pseudotyped vesicular stomatitis virus (VSV) particles expressing luciferase. While all spike mutations slightly increased entry over WT spike on human DPP4 cells, there was a striking
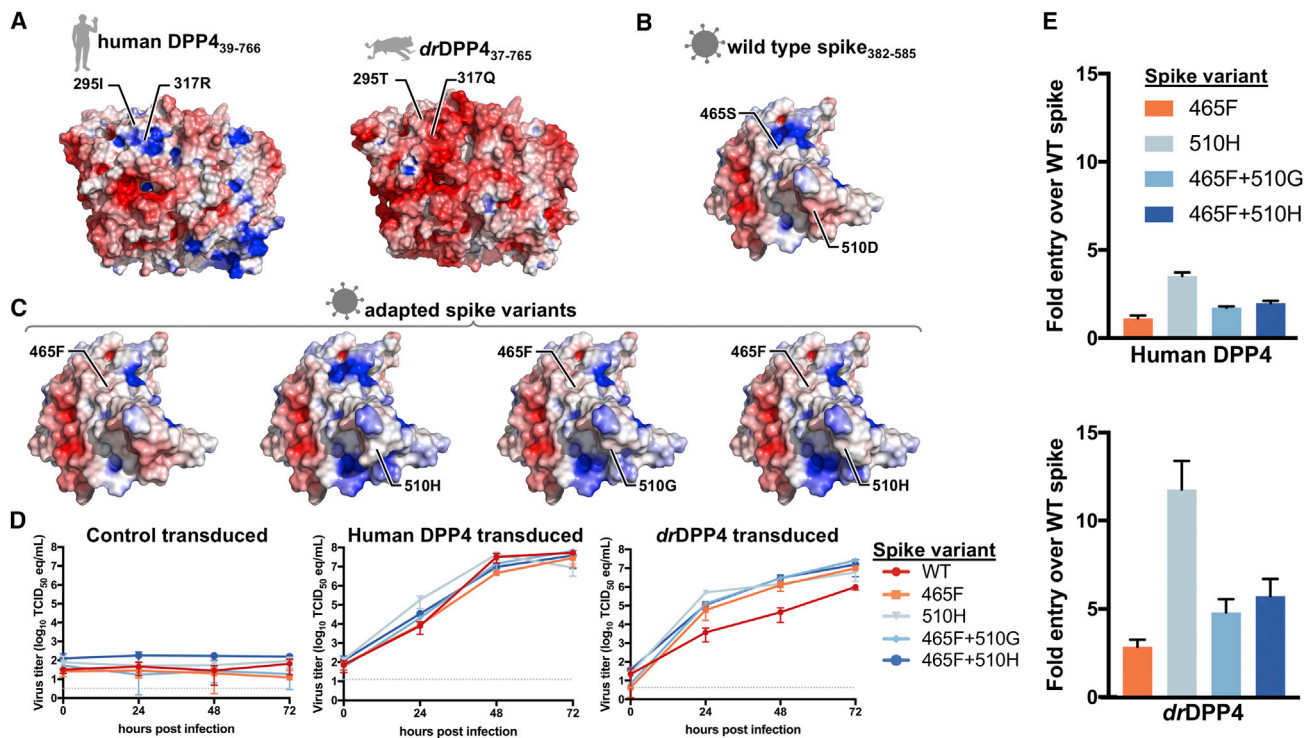
Figure 3. Structural Analysis and Functional Testing of Spike Mutations

(A) Surface charge of human DPP4 (amino acids 39–766; PDB: 4L72) and predicted *dr*DPP4 structure (amino acids 37–765). Residues 295 and 317 are shown. Blue indicates positive charge, red indicates negative charge.

(B) Surface charge of the MERS-CoV spike (amino acids 382–585; PDB: 4L72).

(C) Surface charge of MERS-CoV spike mutations.

(D) DPP4 cells were infected with mutant viruses at MOI = 0.001 and supernatants were collected at the indicated time points. Viral titer was determined qRT-PCR. Error bars represent the SDs of three replicates. See also Figure S4B.

(E) DPP4 transduced cells were infected with spike-pseudotyped VSV-particles and luciferase was measured 24 hr later. Error bars represent the SDs of three replicates.

increase in entry with *dr*DPP4 cells (Figure 3E). Collectively, these findings demonstrate that adaptation in MERS-CoV spike enhanced viral replication on *dr*DPP4 cells through increased viral entry.

Spike Adaptation Specificity

We transfected cells with a subset of the bat DPP4 panel and then infected with spike mutant viruses, all of which replicated better than WT virus on cells expressing *dr*DPP4 (Figure 4). While some mutants performed better than WT virus on cells expressing other bat DPP4s, there was not a consistent top-performing mutant. Notably, spike-510H only replicated better than WT virus with *dr*DPP4 and not the other bat DPP4s, suggesting that this mutation is specific for *dr*DPP4.

DISCUSSION

While numerous studies have shown that MERS-CoV can infect several different species, our understanding of the genetic mechanisms underlying cross species spillover remains unclear (Adney et al., 2014; Agrawal et al., 2015; Cockrell et al., 2016; de Wit et al., 2013; Falzarano et al., 2014; Munster et al., 2016).

Here, we investigated species promiscuity and adaptability of MERS-CoV.

Previous studies have shown that MERS-CoV entry is less efficient with DPP4 from pipistrelle bats compared to human DPP4 (Barlan et al., 2014; Raj et al., 2013; Yang et al., 2014). This difference in receptor efficiency was used to suggest that MERS-CoV spike adapted away from using bat DPP4 as it adapted to human DPP4. While our data confirm this replication phenotype with *Pipistrellus* DPP4, we showed that DPP4 from several other bat species supported MERS-CoV replication comparable to or better than human DPP4 (Figure 1B). Thus, without more evidence as to the true ancestral host of MERS-CoV, conclusions regarding spike adaptation away from bats should be more reserved. This finding also highlights the importance of screening a broad selection of species when assessing host breadth.

A. planirostris and *A. jamaicensis* DPP4s are identical to human DPP4 at the 14 contact points with spike but differed in their ability to support MERS-CoV replication (Figure 1B). Notably, these two bat DPP4 sequences varied from human DPP4 and from each other at other positions in the receptor binding domain (Figure S3B), suggesting that additional DPP4 residues can influence the interaction with spike.
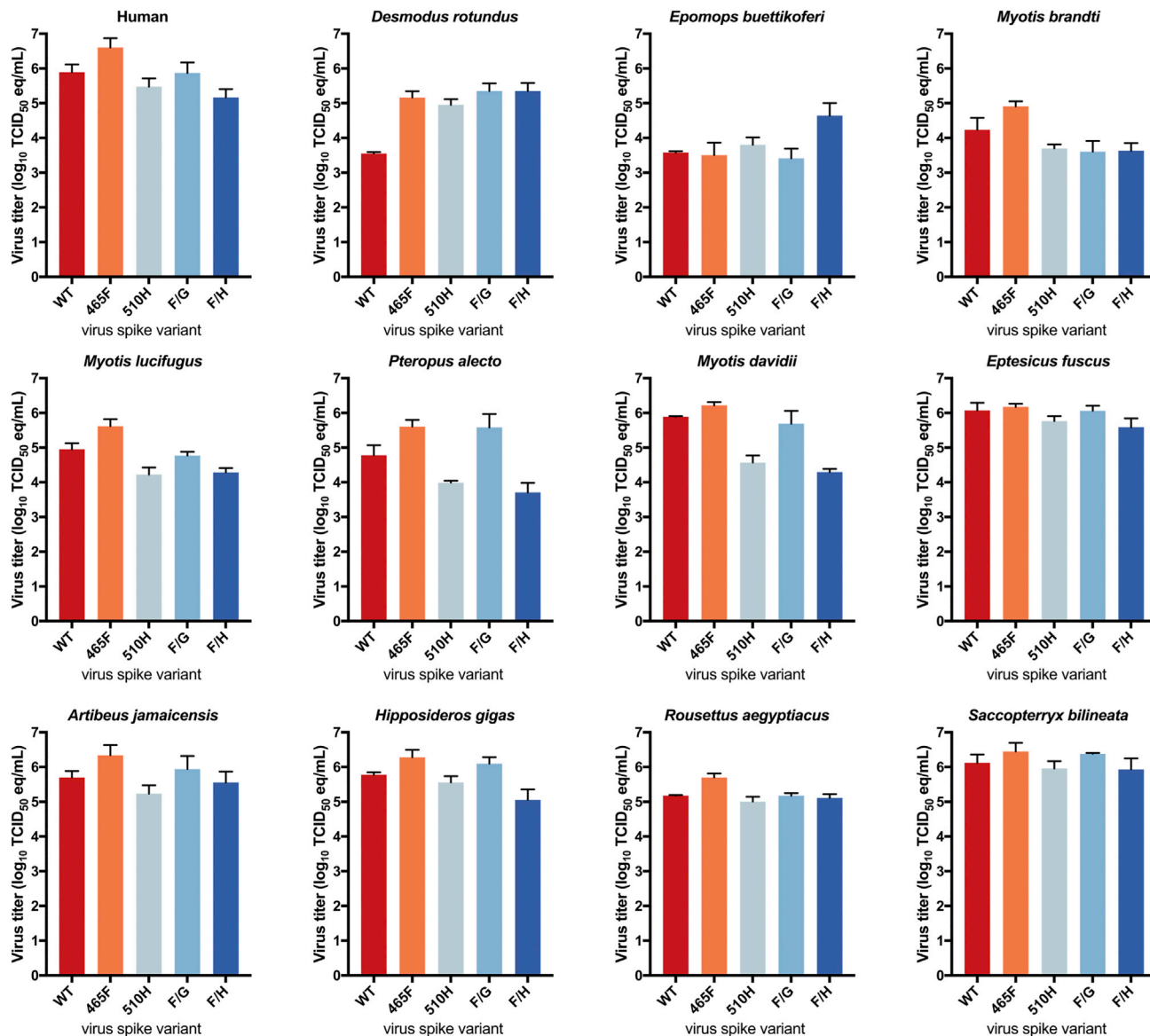
Figure 4. Spike Adaptation Specificity

BHKs were transfected with indicated DPP4s and infected with mutant viruses at MOI = 0.005. Viral titer of supernatants taken at 72 hr was determined by qRT-PCR. Error bars represent SDs of two replicates.

Forced adaptation of MERS-CoV spike has been a challenge in the field as DPP4 from most non-permissive species contains glycosylation that completely abrogates the interaction and blocks infection (Cockrell et al., 2014; Peck et al., 2015; Peck et al., 2017). Without viral replication, it has not been possible to experimentally demonstrate evolution of the MERS-CoV spike. We found that *dr*DPP4 was only semi-permissive to viral infection and, therefore, served as a tool to test MERS-CoV spike adaptation *in vitro* (Figures 1 and 2). Within three passages on cells expressing *dr*DPP4, MERS-CoV accumulated mutations in the receptor-binding domain of spike that enhanced viral entry and replication specifically with *dr*DPP4 and not the other bat DPP4s (Figures 2, 3,

and 4). The prevalence of these adaptation mutations is low in published sequences, further suggesting that they are specific for *dr*DPP4 (Figure S4A). Taken together, MERS-CoV spike is likely adaptable to any DPP4 variation that does not completely ablate the interaction.

At least 14 contact points have been identified in crystal structures of human DPP4 and MERS-CoV spike (Wang et al., 2013). *dr*DPP4 contains variation within and around these known points (Figure S3B). Therefore, the spike-465F mutation, which is just outside of the interface, may lead to broader structural adjustments that favor interaction with *dr*DPP4 (Figure 2H). Surprisingly, the adaptation mutations had very little effect on the interaction with human DPP4, suggesting that other contact points

could compensate for this variation (Figure 3). For example, spike residue 510 has been shown to contact DPP4 residue 322 in addition to 317, so it may be possible that this interaction is retained with human DPP4 (Wang et al., 2013). Structural studies are needed to fully define how these spike mutations influence the interface with DPP4.

Our viral adaptation experiments revealed mutations in MERS-CoV spike, which altered the surface charge to complement the opposite charge of *dr*DPP4 (Figure 3C). Interestingly, these mutations share a striking similarity to species adaptations identified in SARS-CoV spike (as reviewed in Li, 2013). The ability to rapidly adjust surface charge may be a general property of MERS-CoV spike to facilitate cross-species adaptation. However, animal studies are needed to see if the mutations we described here affect other viral phenotypes, including host immune evasion.

Previous work has assessed coronavirus spike adaptation to orthologous host receptors (Baric et al., 1999; McRoy and Baric, 2008; Roberts et al., 2007; Sheahan et al., 2008; Wu et al., 2012). These studies characterized viruses after passage in animals, long-term cell culture, or performed biochemical analysis on spike variations from different isolates. As these experiments only focused on the viral endpoint, they failed to capture the continuous evolution through viral passages. Thus, the exact speed and order in which mutations arise in response to receptors from non-cognate species remain unclear in these studies. The work we present here demonstrates that MERS-CoV rapidly adapts to DPP4 variation and can do so utilizing different mutation paths. While *D. rotundus* is not known to be a host species for MERS-CoV, the use of its semi-permissive DPP4 allowed us to observe, with high temporal resolution, species adaptation of MERS-CoV. All together, these findings shed light on the evolutionary mechanisms underlying MERS-CoV cross-species transmission.

EXPERIMENTAL PROCEDURES

Biosafety Statement
All work with infectious MERS-CoV was approved by the Rocky Mountain Laboratories Institutional Biosafety Committee and performed under biosafety level 3 conditions.

Sequencing of Bat DPP4
cDNA from *E. buettikoferi* and *R. aegyptiacus* were derived from the EpoNi/22.1 and RE06 cell lines, respectively. cDNA was produced from *A. planirostris*, *C. perspicillata*, and *S. bilineata* primary lung tissue and *H. gigas* heart tissue, provided by Dr. Tony Schountz. Dr. Lin-Fa Wang provided cDNA extracted from *R. ferrumequinum* primary kidney tissue. DPP4 was amplified using the iProof High-fidelity PCR kit (Bio-Rad), following the manufacturer's instructions and Sanger sequencing.

Plasmids
DPP4 coding sequences from human (NM001935.3), *A. jamaicensis* (KF574262), *A. planirostris* (MH299895), *C. perspicillata* (MH299896), *D. rotundus* (GABZ01004546.1), *E. buettikoferi* (MH299897), *E. fuscus* (XM008138769), *H. gigas* (MH299898), *M. brandtii* (XM005859372.1), *M.davidii* (XM006766490.1), *M. lucifugus* (XM006083213.1), *P. pipistrellus* (KC249974.1), *P. alecto* (XM006921123.1), *P. vampyrus* (XM011358549), *R. ferrumequinum* (MH299899), *R. aegyptiacus* (MH299900), and *S. bilineata* (MH299901) were synthesized into pcDNA3.1 (Thermo-Fisher). DPP4 was cloned into the lentiviral expression vector provided by Dr. Viviana Simon.

MERS-CoV spike plasmid was provided by Dr. Fang Li. Mutations were introduced into DPP4, pBAC-MERS/EMC12, or the MERS-spike plasmid by overlap PCR.

Viruses
MERS-CoV/EMC12 was propagated as previously described (van Doremalen et al., 2016). The WT virus stock was deep sequenced on the Illumina platform to confirm the absence of mutations described in this study. Mutant viruses were rescued as previously described (Almazán et al., 2013). Titers of all viruses used in this study were determined by endpoint titration in Vero cells as previously described (van Doremalen et al., 2014).

Transfections
Cells were transfected, in 6-well format, with 3 μg of DNA using Lipofectamine 2000 (Life Technologies), following the manufacturer's instructions.

Lentiviral Vectors, Cell Transduction, and Flow Cytometry
Lentiviral particles were produced in 293T cells. Transduced BHKs were placed under 1 μg/mL puromycin selection, as described previously (Letko et al., 2015). Flow cytometry was used to determine mCherry transduction efficiency and DPP4 expression (AF1180, R&D Systems).

Forced Adaptation of MERS-CoV EMC 2012 on Transduced Cells
Human DPP4, *dr*DPP4, and BFP cells were infected with MERS-CoV/EMC12 at an MOI of 0.01 in triplicate. Every 72 hr, 250 μL of supernatant from each replicate was transferred to fresh cell cultures. For each passage, RNA was extracted from supernatant using the QIAamp Viral RNA kit (QIAGEN) and converted to cDNA using SuperScript III (Invitrogen). The spike RBD was amplified and Sanger sequenced. Full-length spike was sequenced for passages 3, 6, and 9.

Structural Modeling and Electrostatic Potential Analysis
The co-structure of MERS-CoV spike and human DPP4 (PDB ID: 4L72 [Wang et al., 2013]) was modeled in Pymol and used to predict the structure for *dr*DPP4 (https://swissmodel.expasy.org). Poisson-Boltzmann analysis was performed with the PDB2PQR server (Dolinsky et al., 2004) and adaptive Poisson-Blotzmann Solver tool extension in Pymol (Baker et al., 2001).

MERS-CoV Replication Kinetics
Viral RNA was extracted from culture supernatants with the QIAamp viral RNA kit (QIAGEN). MERS-CoV titer of cell culture supernatants was determined by endpoint titration on Vero cells (van Doremalen et al., 2016) or qRT-PCR as previously described (Corman et al., 2012).

Pseudotype Entry Assay
Pseudotyped VSV particles were produced as previously described and titered on Vero cells (Takada et al., 1997). BHK-DPP4 cells were infected at an MOI = 1 with pseudotyped particles as previously described (Yang et al., 2014). Luciferase was measured 24 hr post-infection using a firefly luciferase detection kit (Promega) and a Synergy HTX plate reader (Biotek).

Statistical Methods
GraphPad (Prism) was used to analyze quantitative viral titer and viral entry data.

DATA AND SOFTWARE AVAILABILITY

Accession numbers for the novel DPP4 sequences reported in this paper are GenBank: MH299895-MH299901. DPP4 sequence alignment from this study is available via Mendeley Data: https://data.mendeley.com/datasets/232nv29t87/1.

SUPPLEMENTAL INFORMATION

Supplemental Information includes four figures and can be found with this article online at https://doi.org/10.1016/j.celrep.2018.07.045.

AUTHOR CONTRIBUTIONS

M.L., R.M., N.v.D., and V.M. designed experiments. M.L., R.M., K.M., S.N.S., A.C., N.v.D., L.E., and I.S. performed experiments. M.L. wrote the paper. All authors contributed to the study and provided comments on the manuscript.

DECLARATION OF INTERESTS

The authors declare no competing interests.

REFERENCES

Adney, D.R., van Doremalen, N., Brown, V.R., Bushmaker, T., Scott, D., de Wit, E., Bowen, R.A., and Munster, V.J. (2014). Replication and shedding of MERS-CoV in upper respiratory tract of inoculated dromedary camels. Emerg. Infect. Dis. *20*, 1999–2005.

Agrawal, A.S., Garron, T., Tao, X., Peng, B.H., Wakamiya, M., Chan, T.S., Couch, R.B., and Tseng, C.T. (2015). Generation of a transgenic mouse model of Middle East respiratory syndrome coronavirus infection and disease. J. Virol. *89*, 3659–3670.

Almazán, F., DeDiego, M.L., Sola, I., Zuñiga, S., Nieto-Torres, J.L., Marquez-Jurado, S., Andrés, G., and Enjuanes, L. (2013). Engineering a replication-competent, propagation-defective Middle East respiratory syndrome coronavirus as a vaccine candidate. MBio *4*, e00650–13.

Azhar, E.I., El-Kafrawy, S.A., Farraj, S.A., Hassan, A.M., Al-Saeed, M.S., Hashem, A.M., and Madani, T.A. (2014). Evidence for camel-to-human transmission of MERS coronavirus. N. Engl. J. Med. *370*, 2499–2505.

Baker, N.A., Sept, D., Joseph, S., Holst, M.J., and McCammon, J.A. (2001). Electrostatics of nanosystems: application to microtubules and the ribosome. Proc. Natl. Acad. Sci. USA *98*, 10037–10041.

Baric, R.S., Sullivan, E., Hensley, L., Yount, B., and Chen, W. (1999). Persistent infection promotes cross-species transmissibility of mouse hepatitis virus. J. Virol. *73*, 638–649.

Barlan, A., Zhao, J., Sarkar, M.K., Li, K., McCray, P.B., Jr., Perlman, S., and Gallagher, T. (2014). Receptor variation and susceptibility to Middle East respiratory syndrome coronavirus infection. J. Virol. *88*, 4953–4961.

Caì, Y., Yú, S.Q., Postnikova, E.N., Mazur, S., Bernbaum, J.G., Burk, R., Zhāng, T., Radoshitzky, S.R., Müller, M.A., Jordan, I., et al. (2014). CD26/DPP4 cell-surface expression in bat cells correlates with bat cell susceptibility to Middle East respiratory syndrome coronavirus (MERS-CoV) infection and evolution of persistent infection. PLoS ONE *9*, e112060.

Cockrell, A.S., Peck, K.M., Yount, B.L., Agnihothram, S.S., Scobey, T., Curnes, N.R., Baric, R.S., and Heise, M.T. (2014). Mouse dipeptidyl peptidase 4 is not a functional receptor for Middle East respiratory syndrome coronavirus infection. J. Virol. *88*, 5195–5199.

Cockrell, A.S., Yount, B.L., Scobey, T., Jensen, K., Douglas, M., Beall, A., Tang, X.C., Marasco, W.A., Heise, M.T., and Baric, R.S. (2016). A mouse model for MERS coronavirus-induced acute respiratory distress syndrome. Nat. Microbiol. *2*, 16226.

Corman, V.M., Eckerle, I., Bleicker, T., Zaki, A., Landt, O., Eschbach-Bludau, M., van Boheemen, S., Gopal, R., Ballhause, M., Bestebroer, T.M., et al. (2012). Detection of a novel human coronavirus by real-time reverse-transcription polymerase chain reaction. Euro Surveill. *17*, 20285.

de Wit, E., Rasmussen, A.L., Falzarano, D., Bushmaker, T., Feldmann, F., Brining, D.L., Fischer, E.R., Martellaro, C., Okumura, A., Chang, J., et al. (2013). Middle East respiratory syndrome coronavirus (MERS-CoV) causes transient lower respiratory tract infection in rhesus macaques. Proc. Natl. Acad. Sci. USA *110*, 16598–16603.

Dolinsky, T.J., Nielsen, J.E., McCammon, J.A., and Baker, N.A. (2004). PDB2PQR: an automated pipeline for the setup of Poisson-Boltzmann electrostatics calculations. Nucleic Acids Res. *32*, W665-7.

Falzarano, D., de Wit, E., Feldmann, F., Rasmussen, A.L., Okumura, A., Peng, X., Thomas, M.J., van Doremalen, N., Haddock, E., Nagy, L., et al. (2014). Infection with MERS-CoV causes lethal pneumonia in the common marmoset. PLoS Pathog. *10*, e1004250.

Haagmans, B.L., Al Dhahiry, S.H., Reusken, C.B., Raj, V.S., Galiano, M., Myers, R., Godeke, G.J., Jonges, M., Farag, E., Diab, A., et al. (2014). Middle East respiratory syndrome coronavirus in dromedary camels: an outbreak investigation. Lancet Infect. Dis. *14*, 140–145.

Ithete, N.L., Stoffberg, S., Corman, V.M., Cottontail, V.M., Richards, L.R., Schoeman, M.C., Drosten, C., Drexler, J.F., and Preiser, W. (2013). Close relative of human Middle East respiratory syndrome coronavirus in bat, South Africa. Emerg. Infect. Dis. *19*, 1697–1699.

Letko, M., Booiman, T., Kootstra, N., Simon, V., and Ooms, M. (2015). Identification of the HIV-1 Vif and Human APOBEC3G Protein Interface. Cell Rep. *13*, 1789–1799.

Li, F. (2013). Receptor recognition and cross-species infections of SARS coronavirus. Antiviral Res. *100*, 246–254.

Lu, G., Hu, Y., Wang, Q., Qi, J., Gao, F., Li, Y., Zhang, Y., Zhang, W., Yuan, Y., Bao, J., et al. (2013). Molecular basis of binding between novel human coronavirus MERS-CoV and its receptor CD26. Nature *500*, 227–231.

McRoy, W.C., and Baric, R.S. (2008). Amino acid substitutions in the S2 subunit of mouse hepatitis virus variant V51 encode determinants of host range expansion. J. Virol. *82*, 1414–1424.

Munster, V.J., Adney, D.R., van Doremalen, N., Brown, V.R., Miazgowicz, K.L., Milne-Price, S., Bushmaker, T., Rosenke, R., Scott, D., Hawkinson, A., et al. (2016). Replication and shedding of MERS-CoV in Jamaican fruit bats (Artibeus jamaicensis). Sci. Rep. *6*, 21878.

Ohnuma, K., Haagmans, B.L., Hatano, R., Raj, V.S., Mou, H., Iwata, S., Dang, N.H., Bosch, B.J., and Morimoto, C. (2013). Inhibition of Middle East respiratory syndrome coronavirus infection by anti-CD26 monoclonal antibody. J. Virol. *87*, 13892–13899.

Peck, K.M., Cockrell, A.S., Yount, B.L., Scobey, T., Baric, R.S., and Heise, M.T. (2015). Glycosylation of mouse DPP4 plays a role in inhibiting Middle East respiratory syndrome coronavirus infection. J. Virol. *89*, 4696–4699.

Peck, K.M., Scobey, T., Swanstrom, J., Jensen, K.L., Burch, C.L., Baric, R.S., and Heise, M.T. (2017). Permissivity of Dipeptidyl Peptidase 4 Orthologs to Middle East Respiratory Syndrome Coronavirus Is Governed by Glycosylation and Other Complex Determinants. J. Virol. *91*, e00534-17.

Raj, V.S., Mou, H., Smits, S.L., Dekkers, D.H., Müller, M.A., Dijkman, R., Muth, D., Demmers, J.A., Zaki, A., Fouchier, R.A., et al. (2013). Dipeptidyl peptidase 4 is a functional receptor for the emerging human coronavirus-EMC. Nature *495*, 251–254.

Roberts, A., Deming, D., Paddock, C.D., Cheng, A., Yount, B., Vogel, L., Herman, B.D., Sheahan, T., Heise, M., Genrich, G.L., et al. (2007). A mouse-adapted SARS-coronavirus causes disease and mortality in BALB/c mice. PLoS Pathog. *3*, e5.

Sheahan, T., Rockx, B., Donaldson, E., Sims, A., Pickles, R., Corti, D., and Baric, R. (2008). Mechanisms of zoonotic severe acute respiratory syndrome coronavirus host range expansion in human airway epithelium. J. Virol. *82*, 2274–2285.

Song, W., Wang, Y., Wang, N., Wang, D., Guo, J., Fu, L., and Shi, X. (2014). Identification of residues on human receptor DPP4 critical for MERS-CoV binding and entry. Virology *471-473*, 49–53.

Takada, A., Robison, C., Goto, H., Sanchez, A., Murti, K.G., Whitt, M.A., and Kawaoka, Y. (1997). A system for functional analysis of Ebola virus glycoprotein. Proc. Natl. Acad. Sci. USA *94*, 14764–14769.

van Doremalen, N., Miazgowicz, K.L., Milne-Price, S., Bushmaker, T., Robertson, S., Scott, D., Kinne, J., McLellan, J.S., Zhu, J., and Munster, V.J. (2014). Host species restriction of Middle East respiratory syndrome coronavirus through its receptor, dipeptidyl peptidase 4. J. Virol. *88*, 9220–9232.

van Doremalen, N., Miazgowicz, K.L., and Munster, V.J. (2016). Mapping the Specific Amino Acid Residues That Make Hamster DPP4 Functional as a Receptor for Middle East Respiratory Syndrome Coronavirus. J. Virol. *90*, 5499–5502.

Wang, N., Shi, X., Jiang, L., Zhang, S., Wang, D., Tong, P., Guo, D., Fu, L., Cui, Y., Liu, X., et al. (2013). Structure of MERS-CoV spike receptor-binding domain complexed with human receptor DPP4. Cell Res. *23*, 986–993.

World Health Organization. (2018). East respiratory syndrome coronavirus (MERS-CoV). http://www.who.int/emergencies/mers-cov/en/.

Woo, P.C., Lau, S.K., Li, K.S., Tsang, A.K., and Yuen, K.Y. (2012). Genetic relatedness of the novel human group C betacoronavirus to Tylonycteris bat coronavirus HKU4 and Pipistrellus bat coronavirus HKU5. Emerg. Microbes Infect. *1*, e35.

Wu, K., Peng, G., Wilken, M., Geraghty, R.J., and Li, F. (2012). Mechanisms of host receptor adaptation by severe acute respiratory syndrome coronavirus. J. Biol. Chem. *287*, 8904–8911.

Yang, Y., Du, L., Liu, C., Wang, L., Ma, C., Tang, J., Baric, R.S., Jiang, S., and Li, F. (2014). Receptor usage and cell entry of bat coronavirus HKU4 provide insight into bat-to-human transmission of MERS coronavirus. Proc. Natl. Acad. Sci. USA *111*, 12516–12521.

Zaki, A.M., van Boheemen, S., Bestebroer, T.M., Osterhaus, A.D., and Fouchier, R.A. (2012). Isolation of a novel coronavirus from a man with pneumonia in Saudi Arabia. N. Engl. J. Med. *367*, 1814–1820.